Role of 3D SPACE sequence and susceptibility weighted imaging in the evaluation of hydrocephalus and treatment-oriented refined classification of hydrocephalus

Amarnath Chellathurai, Komalavalli Subbiah, Barakath Nisha Abdul Ajis, Suhasini Balasubramaniam, Sathyan Gnanasigamani

Department of Radiodiagnosis, Govt Stanley Medical College, Affiliated to The Tamil Nadu Dr. MGR Medical University, Anna Salai, Guindy, Chennai, Tamil Nadu, India

Correspondence: Dr. Komalavalli Subbiah, Department of Radiodiagnosis, Government Stanley Medical College, Chennai - 600 001, Tamil Nadu, India. E-mail: drkomalarajesh@gmail.com

Abstract

Objective: The aim of our study was to evaluate the diagnostic utility of three-dimensional sampling perfection with application optimized contrast using different flip angle evolution (3D SPACE) sequence and Susceptibility Weighted Imaging (SWI) in hydrocephalus and to propose a refined definition and classification of hydrocephalus with relevance to the selection of treatment option. **Materials and Methods:** A prospective study of 109 patients with hydrocephalus was performed with magnetic resonance imaging (MRI) brain using standardized institutional sequences along with additional sequences 3D SPACE and SWI. The images were independently read by two senior neuroradiologists and the etiopathogenesis of hydrocephalus was arrived by consensus. **Results:** With conventional sequences, 46 out of 109 patients of hydrocephalus were diagnosed as obstructive of which 21 patients showed direct signs of obstruction and 25 showed indirect signs. In the remaining 63 patients of communicating hydrocephalus, cause could not be found out in 41 patients. Whereas with 3D SPACE sequence, 88 patients were diagnosed as obstructive hydrocephalus in which all of them showed direct signs of obstruction and 21 patients were diagnosed as communicating hydrocephalus. By including SWI, we found out hemorrhage causing intraventricular obstruction in three patients and hemorrhage at various sites in 24 other patients. With these findings, we have classified the hydrocephalus into communicating and noncommunicating, with latter divided into intraventricular and extraventricular obstruction, which is very well pertaining to the selection of surgical option. **Conclusion:** We strongly suggest to include 3D SPACE and SWI sequences in the set of routine MRI sequences, as they are powerful diagnostic tools and offer complementary information regarding the precise evaluation of the etiopathogenesis of hydrocephalus and have an effective impact in selecting the mode of management.

Key words: 3D SPACE sequence; communicating hydrocephalus; hemorrhage; membranous obstruction; obstructive hydrocephalus; susceptibility weighted imaging

Access this article online	
Quick Response Code:	Website: www.ijri.org
	DOI: 10.4103/ijri.IJRI_161_18

Cite this article as: Chellathurai A, Subbiah K, Abdul Ajis BN, Balasubramaniam S, Gnanasigamani S. Role of 3D SPACE sequence and susceptibility weighted imaging in the evaluation of hydrocephalus and treatment-oriented refined classification of hydrocephalus. Indian J Radiol Imaging 2018;28:385-94.

Introduction

Hydrocephalus is a disorder of abnormal accumulation of cerebrospinal fluid (CSF) within the ventricles or subarachnoid space due to the imbalance between inflow and outflow of CSF circulation.[1,2] It is the feature of most of the congenital and acquired brain disorders, causing dilatation of the ventricles, which ends up in multiple complications.[2] Frequently, it is caused by ventricular obstruction known as noncommunicating or obstructive hydrocephalus. Other entity is communicating or nonobstructive hydrocephalus due to the interruption in CSF absorption or due to the overproduction of CSF.[3,4]

Current classification of hydrocephalus divides it into noncommunicating and communicating hydrocephalus, the latter is again divided into with cisternal obstruction or without obstruction.[5,6] The surgical modalities now in practice are shunt placement and endoscopic third ventriculostomy (ETV). But, still there exists a confusion in selecting the treatment modality, whether shunt or ETV[5,7]

Magnetic resonance imaging (MRI) remains the primary imaging modality for the initial evaluation of these patients, because it effectively allows detection and differentiation of various etiologies of hydrocephalus.[8] Despite its sensitiveness, it falls short of exploring some hidden causes of hydrocephalus with routinely used conventional sequences. It fails to elucidate thin membranes causing obstruction as well as small hemorrhages associated with hydrocephalus.[9]

Three-dimensional sampling perfection with application optimized contrast using different flip angle evolution (3D SPACE) sequence is an advanced MRI technique which is gaining popularity as a sensitive imaging modality in hydrocephalus especially obstructive, because it permits more precise identification and localization of very thin membranes and provide useful information regarding the level of obstruction.[9,10] 3D SPACE sequence also plays a role in communicating hydrocephalus as in tuberculous meningitis, which is very common in developing countries such as India, by detecting the altered signal intensity to loss of signal intensity in the basal cisterns by inflammatory cells.[11] It is a modification of 3D turbo spin echo sequence where the whole imaging volume is excited so that the images can be reconstructed in multiple planes. It uses radiofrequency pulses with variable flip angles, which are nonselective, short refocusing pulse trains with very high turbo factors, and high sampling efficiency. SPACE sequence can produce high-resolution isotropic images and are less sensitive to flow, chemical shift, and susceptibility artifacts.[9,10]

Susceptibility Weighted Imaging (SWI) is another advanced MRI technique that demarcates the exact site and size of the hemorrhage clearly. It is a 3D velocity compensated gradient echo MRI sequence, which evaluates and exploits the differences in the magnetic susceptibility of various tissues for obtaining an image.[12,13] SWI is obtained as magnitude or phase images and combination of these two. The major advantage we can utilize from this sequence is that it can differentiate hemorrhage from calcification, which we cannot expect in any other sequence, even in gradient.[14]

To the best of our knowledge, only a few studies are there in the literature regarding the role of 3D SPACE sequence, and there is no study regarding SWI in the assessment of hydrocephalus. In this study, we explore the diagnostic utility of 3D SPACE sequence and SWI in hydrocephalus and based on those findings, and we propose a simpler and refined definition and classification of hydrocephalus, which would satisfy the selection of treatment option.

Materials and Methods

This prospective study was conducted in our institute from January 2014 to December 2017. Approval was obtained from the ethical committee. Patients with hydrocephalus who were referred for MRI brain were enrolled for our study. We included 109 patients with moderate to severe hydrocephalus based on Evans index. We excluded patients >50 years (due to age related dilatation of ventricles), normal pressure hydrocephalus, those patients with brain atrophy or ex-vacou dilatation, and those who were on treatment or undergone shunt procedures or other surgeries. Informed consent was obtained from all patients or caregivers.

MRI brain was done using Siemens Magnetom Aera 48 Channel 1.5 Tesla Machine (Germany) using standardized institutional protocol, including T1W sagittal, T2W axial, FLAIR coronal, diffusion weighted image with ADC mapping, gradient, MRA/MRV, and postcontrast study (if needed). The additional sequences we included were as follows: 3D SPACE sequence and SWI. 3D SPACE sequence was obtained in a sagittal plane covering all the ventricles and cisterns.

MRI protocol for 3D SPACE and SWI was shown in Table 1.

Analysis

The conventional images were reviewed independently by two senior neuroradiologists with 10-year experience. Another two neuroradiologists with same experience analyzed the special sequences. Comprehensive anatomy of each CSF compartment and their hydrodynamics were studied with due care and the etiopathogenesis of hydrocephalus was arrived by consensus. Out of 109 patients, 58 were male and 51 were female. About 42 patients were under the age of 10 years, 39 were between

10 and 20 years, 21 were between 20 and 40 years, and 7 were between 40 and 50 years [Table 2].

The analysis was performed in a step-by-step manner. In the first step, conventional sequences were analyzed carefully for any obstruction and were divided into communicating and noncommunicating hydrocephalus. Our diagnostic criteria for obstructive hydrocephalus were based on direct or indirect signs. Direct sign of obstruction was direct visualization of membrane, mass, hemorrhage, or any other cause leading to obstruction. Indirect signs were proximal upstream dilatation of ventricles, bulging of the CSF fluid just proximal to the level of obstruction, and signal intensity change in proximal and distal sites of obstruction. Accordingly with conventional sequences, we had 63 patients of communicating and 46 patients of noncommunicating hydrocephalus.

Next step was analysis of 3D SPACE sequence in which careful scrutinization of every image was done. All CSF pathways, especially all possible areas of obstruction were examined with caution using 3D multiplanar reconstruction and maximum and minimum intensity projection. The membranes causing obstruction were followed to their full extent and again classified as obstructing and nonobstructing membranes. The obstructing membranes were those, which divide the space into two or more compartments. Using this sequence, 88 patients were diagnosed to have noncommunicating hydrocephalus. Of these 88 patients, 80 patients showed intraventricular obstruction, whereas 8 patients showed extraventricular obstruction. Remaining 21 patients showed communicating hydrocephalus.

Third step was the analysis of SWI to locate the areas of hemorrhage by examining phase, magnitude, combined, and MIP images. In SWI, 3 patients showed intraventricular hemorrhage (cerebral aqueduct and foramen of Magendie) causing obstructive hydrocephalus and 24 patients showed hemorrhage at various sites (both intraventricular and extraventricular). The percentage of communicating and noncommunicating hydrocephalus in these sequences was compared with conventional sequences as shown in Tables 3 and 4.

Diagnostic accuracy was calculated for conventional sequence, 3D SPACE sequence, and SWI and was compared.

Results

Out of 46 noncommunicating hydrocephalus diagnosed by conventional sequences, direct obstruction was seen in 21 patients and indirect signs of obstruction were seen in 25 patients. Direct obstruction included aqueductal membranes in two patients, tectal glioma in one patient, pineal tumor in two patients, Arnold Chiari malformation

Table 1: MRI protocol for 3D SPACE sequence and SWI

Parameters	SWI	3D SPACE
Repetition time (m)	58	3000
Echo time (ms)	40	526
Slice thickness (mm)	1	0.7
Field of view (mm)	230	230
Matrix	256	256
Voxel size	0.7	0.7
Number of signal averaging	2	2
Flip angle (°)	20	100

MRI=Magnetic resonance imaging, 3D SPACE=Three-dimensional sampling perfection with application optimized contrast using different flip angle evolutions, SWI=Susceptibility weighted imaging

Table 2: Age distribution in our study

Age group (years)	Number of patients
0-10	42
10-20	39
20-30	13
30-40	8
40-50	7
Total	109

Table 3: Conventional sequences versus 3D SPACE

Type of hydrocephalus	Conventional sequence	3D SPACE
Communicating hydrocephalus	63 (57.7%)	21 (19.2%)
Non communicating hydrocephalus	46 (42.2%)	88 (80.7%)
With intraventricular obstruction		80 (73.7%)
With extraventricular cisternal obstruction		8 (7.3%)
Total	109 (100%)	109 (100%)

3D SPACE=Three-dimensional sampling perfection with application optimized contrast using different flip angle evolutions

Table 4: Hemorrhages detected in conventional sequences versus SWI

Type of hydrocephalus	Conventional sequence	SWI
Communicating hydrocephalus	2 (1.8%)	9 (8.2%)
Non communicating hydrocephalus	4 (3.6%)	18 (16.5%)
Total number of hemorrhages detected	6 (5.5%)	27 (24.7%)

in four patients, and achondroplasia in one patient. Lilliquist membrane was seen in one patient but was only partially visualized and could not be traced to its full extent. Colloid cyst causing obstruction of foramen of Monro was seen in one patient. One patient of Dandy Walker variant and one patient of Blake pouch cyst were also seen. Arachnoid cyst causing obstruction of fourth ventricle was detected in two patients. Medulloblastoma causing obstruction of fourth ventricle was seen in one patient. Metastasis was seen in four patients out of which two patients showed hemorrhage.

Out of 63 communicating hydrocephalus diagnosed, 14 patients were diagnosed as tuberculous meningitis,

3 patients as encephalitis, and 1 patient as leptomeningeal carcinomatosa. Subarachnoid hemorrhage was seen in two patients and choroid plexus tumor was seen in two patients. The cause of hydrocephalus could not be found in 41 patients with conventional imaging and also we could not find any obstruction in these cases. In three patients, incomplete membranes were seen in grossly dilated lateral ventricles. In two patients, hemorrhage was seen in germinal matrix region, but we could not find its complete extension.

In all 88 noncommunicating hydrocephalus detected by 3D SPACE sequence, the causes of obstruction was seen directly. Overall 49 patients showed membranous obstruction (32 at the level of aqueduct [Figure 1], 7 at the foramen of Magendie, 2 at the level of Lushka, 1 at the level of foramen of Monro, and Lilliquist membrane was seen in 7 patients [Table 5]), 1 patient showed severe narrowing without membrane in bilateral foramen of Monro [Figure 2], 1 patient showed a tiny tumor at the level of aqueduct [Figure 3], 3 patients showed multiple levels of obstruction seen in both aqueduct and outlet of fourth ventricle giving the appearance of trapped ventricle [Figure 4], and in another patient of postmeningitis hydrocephalus, there were multiple septations and synechia causing multicompartmental obstructive hydrocephalus [Figure 5]. Other patients of obstructive hydrocephalus showed the similar findings as in conventional sequences.

In addition to the above said findings, 37 patients of chronic hydrocephalus showed multiple membranes in grossly dilated lateral ventricles, which did not seem to be causing obstruction to the flow. Similar membranes were seen in dilated third ventricle in 13 patients, in fourth ventricle in 2 patients, and in prepontine cistern in 1 patient. These membranes were seen in both communicating as well as noncommunicating hydrocephalus, significance, and pathology of which are uncertain. Thus, in total, we detected 102 membranes by using 3D SPACE sequence.

In cases of turbulent flow of CSF in cerebral aqueduct and outlet of fourth ventricle, 3D SPACE demonstrated flow void in 21 patients [Figure 6], but in conventional sequences, it was seen merely in 2 patients. All the above findings were confirmed during surgery.

SWI detected hemorrhage in 27 patients (hemorrhage at the level of aqueduct in 2 patients, foramen of Magendie in 1 patient, chronic subarachnoid hemorrhage in 8 patients, germinal matrix hemorrhage with intraventricular extension in 6 patients [Figure 7], isolated lateral ventricular hemorrhage in 3 patients, multiple hemorrhagic foci throughout cerebral hemisphere and brainstem in 1 patient of hemorrhagic encephalitis [Figure 8], hemorrhage in 2 primary tumors (1 glioma and 1 medulloblastoma), and hemorrhage in 4 patients of metastasis. SWI detected 27 patients (24.7%) of hemorrhage in contrast to conventional sequence, which detected only 6 patients (5.5%) as shown in Table 6. The causes of hydrocephalus in our study are enumerated in Table 7.

Among 88 patients of obstructive hydrocephalus, 54 were male and 44 were female. And out of 21 communicating hydrocephalus, 9 were male and 12 were female [Table 8].

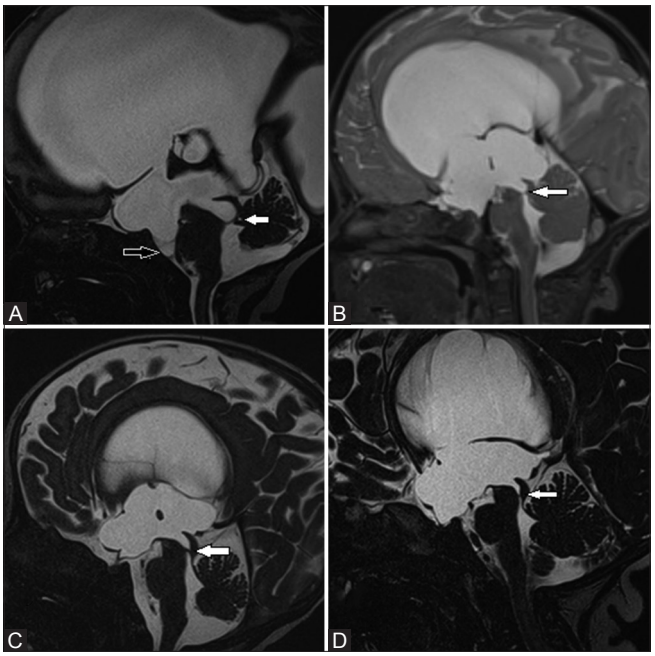

Figure 1 (A-D): (A-D) Sagittal sections of three-dimensional sampling perfection with application optimized contrast using different flip angle evolution sequence in four different patients showing membrane in the cerebral aqueduct causing triventricular hydrocephalus (solid arrows). Also, there is a Lilliquist membrane in one patient (A) in the prepontine cistern (open arrow)

Table 5: Sites of membranous obstruction on conventional and 3D SPACE sequences

Sequences	Localization of obstructive membranes											Total number of membranes
	Obstructive membranes						Nonobstructive membranes					
	Cerebral aqueduct	Foramen of Magendie	Foramina of Luschka	Foramen of Monro	Lilliquist memb rane	Total	Lateral vent ricles	Third vent ricle	Fourth vent ricle	Cisterns	Total	
Conven tional sequences	2	0	0	0	1	3	3	0	0	0	3	6
3D SPACE	32	7	2	1	7	49	37	13	2	1	53	102

3D SPACE=Three-dimensional sampling perfection with application optimized contrast using different flip angle evolutions

Table 6: Sites of hemorrhage detected on conventional sequences and SWI

Sequence	Localization of hemorrhages							Total number of hemorrhage
	Cerebral aqueduct	Foramen of Magendie	Sub arachnoid hemorrhage	Isolated lateral ventricular hemorrhage	Germinal matrix hemorrhage with intraventricular extension	Primary tumor/ metastasis	Encephalitis	
Conventional sequence	0	0	2	0	2	2	0	6
SWI	2	1	8	3	6	6	1	27

SWI=Susceptibility weighted imaging

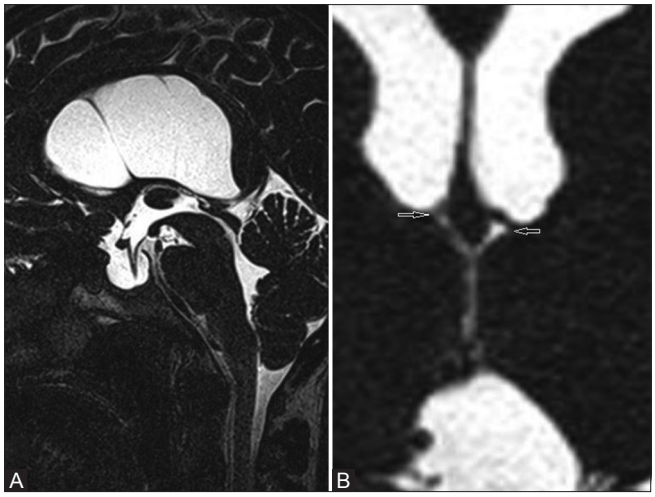

Figure 2 (A and B): (A) Sagittal and (B) coronal sections of three-dimensional sampling perfection with application optimized contrast using different flip angle evolution sequence in a patient showing bilateral foramen of Monro narrowing (arrows) causing upstream dilatation of both lateral ventricles. Also, multiple nonobstructing membranes are seen in lateral ventricles (A)

When compared with conventional sequence, the diagnostic accuracy of 3D SPACE sequence in obstructive hydrocephalus is 100% (Vs 61.4%). In nine patients of communicating hydrocephalus, etiology was detected by SWI, and in three patients of noncommunicating hydrocephalus, level of obstruction was detected using SWI with 95% confidence interval. Thus, SWI is more accurate in obtaining the etiology in communicating hydrocephalus but plays a less role in noncommunicating hydrocephalus.

Discussion

Hydrocephalus is a very common clinical disorder, and effective surgical treatment options are available according to the etiology. The success of these treatment strategies solely depends on the accurate diagnosis and classification of this disorder.[5,7] In literature, as aqueductal stenosis is most common cause of obstructive hydrocephalus, most of the imaging modalities are oriented toward diagnosing this.[8] However, a significant number of patients with other cause of obstructive hydrocephalus are still misdiagnosed as communicating and offered ineffective treatment option.[9] Over the years, advancement of MRI has helped in better understanding of CSF morphology and flow.

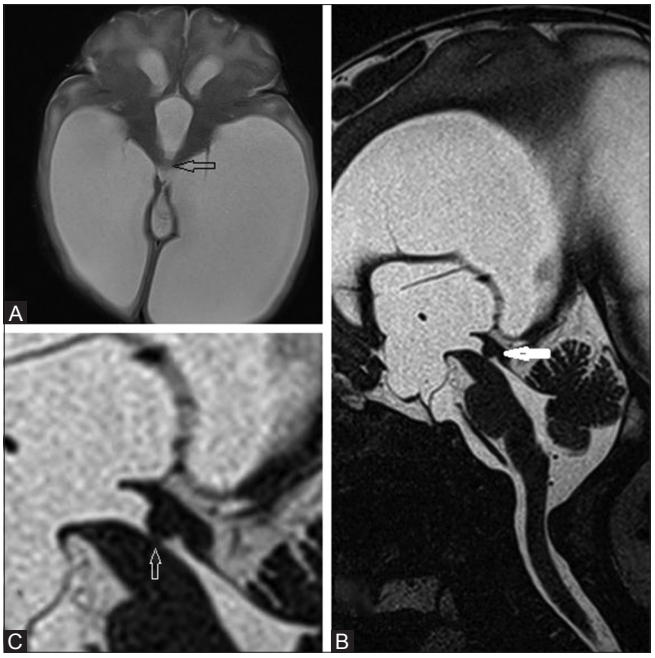

Figure 3 (A-C): (A) T2 weighted axial section in a patient with hydrocephalus showing indirect signs of obstruction at the level of aqueduct (black arrow). (B) Sagittal section of three-dimensional sampling perfection with application optimized contrast using different flip angle evolution sequence showing a tiny tumor (big arrow) at the level of aqueduct which is not visualised in T2WI. (C) Magnified view of the tumor (open white arrow) at the level of aqueduct

Recently, 3D SPACE sequence has been proposed as rapid and most efficient sequence for evaluating hydrocephalus.[10] This is because of their effectiveness in detecting thin membrane as the cause of obstruction and better localization of obstruction. In our study, noncommunicating hydrocephalus were detected in 80.7% of the whole cohort in contrast to 42.2% in conventional sequence. This is mainly because of the insensitive conventional sequence in detecting obstructive causes like thin membranes giving a spurious result of large number of communicating hydrocephalus. We found that the obstructive membranes are not only at the aqueductal level but also at the outlets of fourth ventricle, foramen of Monro, and in the anterior perimesencephalic cistern as well as more membranes [49 obstructing and 53 nonobstructing membranes (total 102) versus 3 obstructing and 3 nonobstructing membranes (total 6)] detected than in conventional sequence. Additionally, it helped in detecting small to very small obstructive lesions,

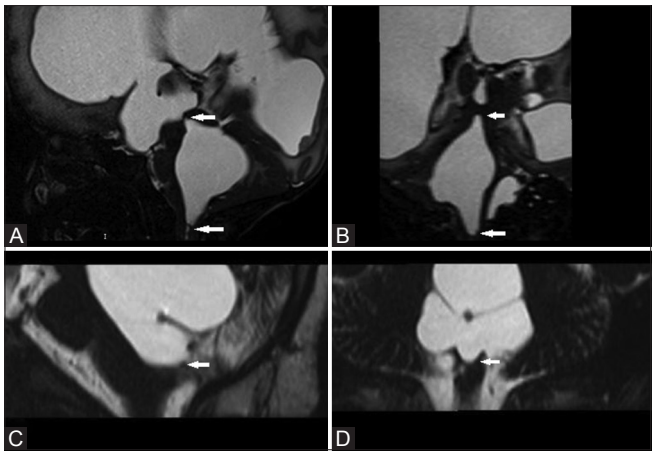

Figure 4 (A-D): Trapped fourth ventricle in two different patients (A and B) and (C and D). (A and B) are three-dimensional sampling perfection with application optimized contrast using different flip angle evolution (3D SPACE) sagittal and coronal sections of a patient showing obstruction at the level of aqueduct and Foramen of Magendie (arrows). Upper arrow in (A) shows aqueductal membrane. Also note the gross dilatation of lateral and third ventricle. (C and D) are 3D SPACE sagittal and coronal sections of another patient showing trapped fourth ventricle, (arrows) showing fourth ventricular outlet obstruction

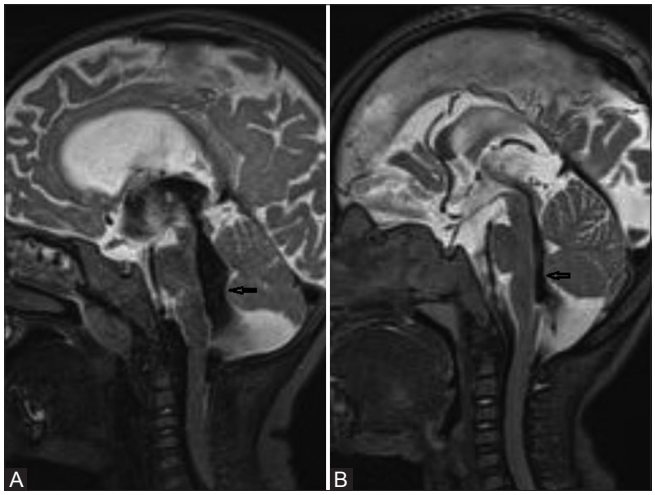

Figure 6 (A and B): (A and B) Sagittal sections of three-dimensional sampling perfection with application optimized contrast using different flip angle evolution sequence in two different patients showing prominent flow void at the level of aqueduct and fourth ventricle (arrows) due to turbulent flow

which were missed in conventional sequence. Recently, this special sequence was found to sensitive in detecting tuberculous meningitis as a cause for communicating hydrocephalus, by detecting altered signal intensity or obliteration of CSF signal intensity in basal cisterns by inflammatory cells. Though rarely reported in western countries, this is a common entity in developing countries such as India.

The prospective study by Dincer *et al*.[9] in 2009 showed 3D-CISS sequences to be more sensitive in diagnosing obstructive hydrocephalus than conventional sequence by

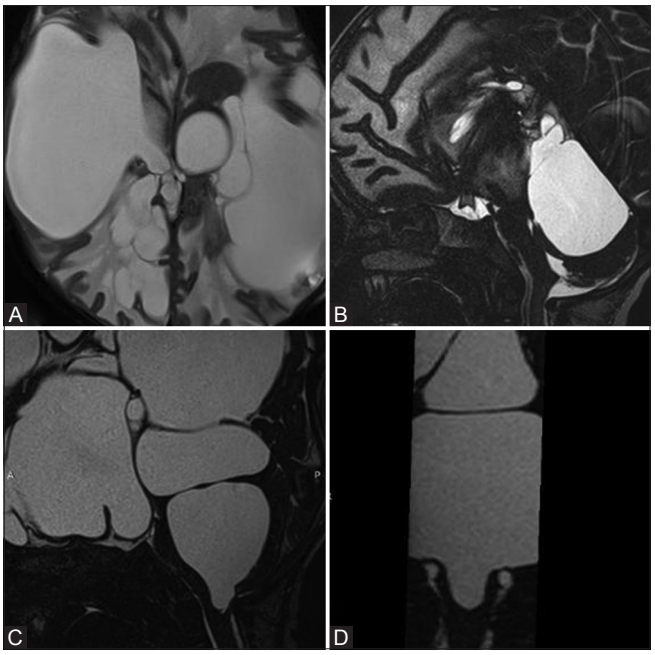

Figure 5 (A-D): (A and B) Multicompartmental obstructive hydrocephalus in a patient with postmeningitis sequel, showing multiple membranes and synachia. (C and D) On follow-up after 18 months, there was an increase in the membranes with complete obstruction of fourth ventricular outlet

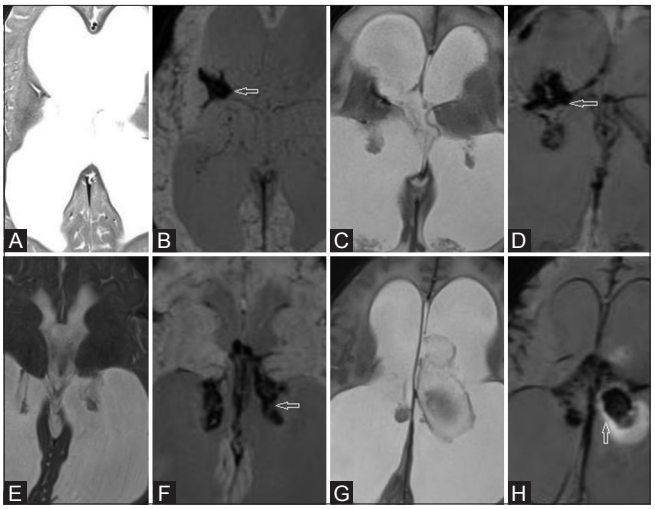

Figure 7 (A-H): T2 weighted axial and susceptibility weighted imaging (SWI) images of four different patients showing hemorrhage, (A and B) SWI showed hemorrhage in right germinal matrix with intraventricular extension (arrow), which is not visible in T2WI. (C and D) another patient showing right germinal matrix hemorrhage with intraventricular extension in SWI (arrow) but T2WI shows a small area of hemorrhage in the germinal matrix, extension into ventricle is not visualised. Another two patients (E and F) and (G and H) show choroid plexus hemorrhage in SWI (arrows) which is not clear on T2WI

diagnosing 19.4% new cases. However, in our study, 47.7% of new obstructive cases out of 109 patients explaining the fact that 3D SPACE has higher resolution than 3D CISS. Similar to our study, Murat Ucar *et al*. in 2014 found that 3D-SPACE yielded less artifacts and high CNR values between the CSF and parenchyma than 3D-CISS.[15,16] Algin

Table 7: Causes of hydrocephalus in our study

Site	Causes	No of patients
Cerebral aqueduct	Membrane	32
	Pineal/tectal tumor	3
	Aqueductal tumor	1
	Hemorrhage	2
Foramen of Magendie and Lushka	Stenosis	
	Membrane	7 (Magendie) + 2 (Lushka)
	Congenital causes - Dandy walker + Arnold chiari + achondroplasia	2 + 4 + 1
	Arachnoid cyst	2
	Hemorrhage	1
Foramen of Monro	Stenosis	1
	Membrane	1
	Colloid cyst occlusion	1
Subarachnoid space	Lilliquist membrane	7
	Hemorrhage	8
	Meningitis	14
	Encephalitis	3
	Leptomeningeal carcinomatosa	1
Intraventricular	Extension from germinal matrix and intracranial hemorrhage	6
	Isolated lateral ventricular hemorrhage	3
	Choroid plexus tumors	2
Parenchymal	Metastasis	4
	Medulloblastoma	1
Total		109

Table 8: Hydrocephalus in male versus female

Hydrocephalus	Male	Female	Total
Non communicating	49	39	88
Communicating	9	12	21
Total	58	51	109

et al. in 2017 stated that 3D-SPACE technique at 3T MRI better delineates the morphology of CSF containing spaces, CSF-related tiny membranes, CSF hydrodynamics, and other associated findings and recommended its routine use for patients with CSF disorders.[17] Our study proved the same.

Algin *et al*. in 2012 evaluated the aqueductal patency of 21 clinically suspicious patients of aqueductal stenosis and 12 control subjects with phase contrast MRI and 3D-SPACE images. 3D space sequence detected stenosis in all patients in which PC MR showed obstructed flow.[10] This study revealed an excellent correlation between 3D-SPACE and PC-MRI. In our study, 32 patients of aqueductal obstruction were diagnosed in contrast to 13 patients using conventional sequences. Moreover, in cases of turbulent flow of CSF in cerebral aqueduct and outlet of fourth ventricle, 3D SPACE sequence was comparable to the sensitiveness of phase contrast MRI, which is the gold standard for CSF flow studies.

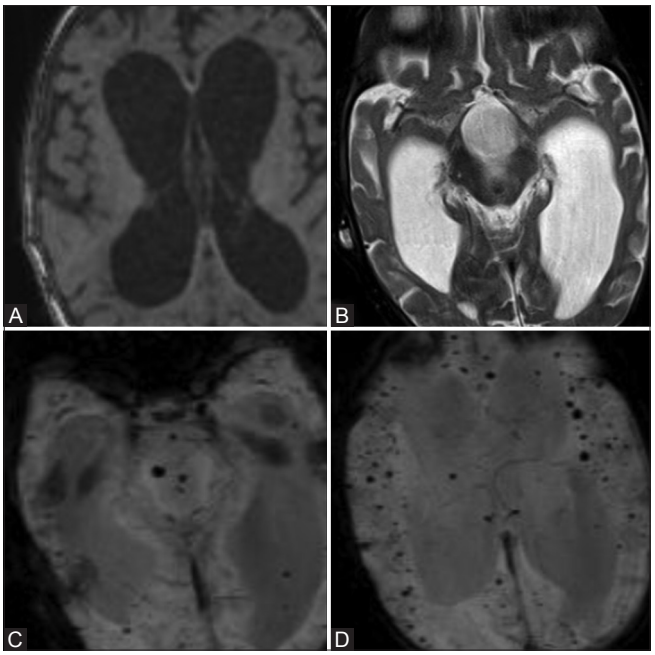

Figure 8 (A-D): T1 WI axial (A), T2I axial (B), susceptibility weighted imaging (SWI) images (C and D) of a patient with hemorrhagic encephalitis; SWI shows multiple tiny hemorrhagic foci in cerebral hemispheres and brainstem, which are not visible in T1 and T2WI images

As intracranial hemorrhage may also be a cause for obstructive hydrocephalus, we added SWI sequence which has higher sensitivity to susceptibility effects and better visualization of the internal architecture of hemorrhagic foci.[13,18,19] Our study supports this by detecting hemorrhage in 27 patients when compared with 6 patients detected by conventional sequence. In few of them, it was found as the cause of obstruction, at aqueduct and rarely at foramen of Magendie. SWI sequence in our study, also detected germinal matrix hemorrhage and chronic subarachnoid hemorrhage as the cause for hydrocephalus in few patients, for which no previous studies were available to compare.

In 1914, Walter Dandy and Blackfan defined hydrocephalus as merely a symptomatic designation and classified into communicating and noncommunicating.[3] Russell *et al*. in 1949 classified it as obstructive and nonobstructive hydrocephalus.[4] Surgical management is the therapeutic option of choice as medical management offers only temporary relief.[5] For communicating hydrocephalus, the standard surgical treatment is shunt placement[7] in the lateral ventricle with different drainage points – ventriculoperitoneal (most common), ventriculopleural, and ventriculoatrial shunt and lumboperitoneal shunt, the drainage point is lumbar intradural space. For obstructive hydrocephalus, ETV is the treatment of choice especially with aqueductal stenosis.[7,20] It is contraindicated in communicating hydrocephalus. Other endoscopic procedures available are fenestration of cysts, foraminoplasty, and marsupialization. Cerebral aqueductoplasty is an effective treatment for

membranous and short-segment stenoses of the sylvian aqueduct.[20] Alternatives treatments, choroid plexectomy or choroid plexus coagulation are effective in cases of CSF over-production. In tumor causing obstruction, removal of tumor cures the hydrocephalus in 80%.[21]

Thus, shunt procedures should be done only in communicating hydrocephalus and in those whose arachnoid villi cannot absorb CSF adequately. For obstructive hydrocephalus, where absorption of CSF is good, the endoscopic procedures are the treatment of choice. Even though a lot of treatment options exist, already existing classification systems pose a difficulty in arriving at a conclusion regarding the option of treatment for the particular type of hydrocephalus. Shunt procedures are done for obstructive hydrocephalus too nowadays increasing the morbidity and mortality due to complications.[5,9,22] So, there is an obligatory need for an exemplary terminology and thoroughgoing flawless classification. Based on our study, we propose a simpler and refined definition and classification, which is the modification of previous ones, pertaining to the selection of surgical options.

We define hydrocephalus as "an active process of fluid accumulation in brain due to imbalance between inflow and outflow of CSF caused by disturbed CSF dynamics, either at the level of secretion, absorption or at any level of circulation." The classification is based on the site of disturbance of CSF dynamics. If the pathology involves the secretion or absorption site of CSF, it is classified as communicating hydrocephalus (inception and termination). Secreting hydrocephalus involves the true communicating hydrocephalus, whereas absorptive hydrocephalus is an obstructive hydrocephalus at the level of end absorption and included in the communicating hydrocephalus due to difference in the treatment. In between these two sites, wherever the pathology resides, it will affect the circulation only. When the circulation is disturbed, it is obviously obstruction to its flow. So, they are grouped as obstructive or noncommunicating hydrocephalus. The classification is summarized in Table 9.

In our classification of communicating hydrocephalus, there is no role for ETV since the absorption of CSF itself is affected. Also, in secretory type of communicating hydrocephalus, overproduction of CSF will be there which could not be completed by the normal rate of absorption. Thus, there is either a need of extracranial CSF diversion or eviction of the cause. In our study population, for communicating hydrocephalus, shunting was done. In obstructive hydrocephalus explained by us, endoscopic procedure will be the first modality of treatment either it can be endoscopic fenestration or third ventriculostomy or marsupialization. In our study, all these patients were treated with one of the above endoscopic procedures according to the cause. Also, 39 patients (35.7%) would have been otherwise treated with ventriculoperitoneal shunt without 3D SPACE diagnosis.

Table 9: Proposed treatment oriented classification of hydrocephalus with etiopathogenesis and options of treatment

Type of hydrocephalus	Goals of Treatment	Level of pathology	Causes	Pathology	Treatment option
Communicating hydrocephalus (pathology at inception and termination of CSF) Secreting and Absorptive hydrocephalus	Control of secretion and improvement of drainage	At the level of secretion (choroid plexus and minor secretory pathway)	Choroid plexus tumor	Carcinoma/papilloma	Tumor resection
			Choroid plexus hyperplasia	Difuse villous hyperplasia	Endoscopic coagulation of choroid plexus
			Idiopathic (rare)	Impaired regulatory mechanism of secretion of CSF	VPS or VAS along with coagulation of choroid plexus
		At the level of absorption (Arachnoid or pacchioni's granulations)	Subarachnoid hemorrhage	Plugging of arachnoid villi by clot and later by scarring and fibrosis	VPS or VAS
			Meningitis (TB and others) and other CNS infection	Plugging of arachnoid villi by inflammatory cells and later by fibrosis and scarring	VPS or VAS
			Normal pressure hydrocephalus	Reduced CSF resorption due to elevated superficial venous pressure which in turn elevates pressure gradient to reabsorb CSF.	VPS or VAS
			Increased venous pressure in dural sinuses or jugular vein due to other causes like thrombosis	Prevents absorption	VPS or VAS
			Congenital absence of arachnoid villi (very rare)	No absorption	VPS or VAS

Contd...

Table 9: Contd...

Type of hydrocephalus	Goals of Treatment	Level of pathology	Causes	Pathology	Treatment option
Noncommuniating hydrocephalus (pathology of the circulation of CSF - obstruction to the intra or extraventricular flow) Obstructive hydrocephalus of CSF circulatory pathway	Removal of the barrier to the flow of CSF	With ventricular obstruction (ventricular obstruction by intra ventricular and extrinsic causes) (primary or secondary)	Aqueduct: Primary aqueductal stenosis Aqueductal membrane Hemorrhage Secondary to parenchymal tumor Arnold chiari	Triventricular hydrocephalus Severe narrowing without membrane Congenital/acquired due to postinfection or post hemorrhage Causing obstruction of passage Causing obstruction of passage Causing obstruction of passage	ETV ETV ETV Resection of tumor/ETV±biopsy ETV±decompression of posterior fossa
			Fourth ventricular outlet - Foramen of Magendie and Lushka Membranous obstruction Hemorrhage Retrocerebellar cyst or tumor Dandy walker malformation Arnold Chiari Other developmental malformations	Tetraventricular hydrocephalus Congenital/acquired due to postinfection or post hemorrhage Obstruction of passage Posterior fossa cyst causing obstruction Obstruction of passage Crowding of posterior fossa Premature skull fusion/brain malformations	ETV+aspiration of hematoma ETV/Endoscopic fenestration of cyst into ventricles/cisterns or marsupialization Endoscopic procedure±decompression
			Foramen of Monro Stenosis Membrane Lesion (colloid cyst/CNC)	Asymmetrical if unilateral Congenital Congenital/acquired due to postinfection or post hemorrhage Obstruction of passage	Endoscation of fenestration of septum pellucidum/monroplasty Excision of cyst
			Others: Intracerebral/germinal matrix hemorrhage with intraventricular extension Any SOL causing obstruction Isolated lateral ventricular hemorrhage		ETV Resection of SOL +/- ETV (if unresectable) Endoscopic fenestration of septum pellucidum
		With extra ventricular cisternal CSF pathway obstruction	Basal cisterns Chronic meningitis Chronic hemorrhage	Due to the formation of obstructing membranes/synechiae	Endoscopic fenestration of membranes
			Subarachnoid space Chronic meningitis Chronic hemorrhage Leptomeningeal carcinomatosa Membranes: Lilliquist membrane Other unnamed membranes	Due to the formation of obstructing membranes/synechiae Causing obstruction of flow in SAS In prepontine cistern below third ventricle-obstruction Obstruction	ETV if in anterior perimesencephalic cistern or endoscopic removal of membrane/synechiae. Chemotherapy ETV with fenestration of membrane Endoscopic fenestration of membrane.

CSF=Cerebrospinal fluid, CNS=Central nervous system, VPS=Ventriculoperitoneal shunt, VAS=Ventriculoatrial shunt, ETV=Endoscopic third ventrculostomy, SOL=Space occupying lesion

Conclusion

3D SPACE sequence in hydrocephalus patients are very sensitive in differentiating obstructive from communicating hydrocephalus, thereby selecting more patients as candidates for endoscopic procedures and reducing the need and complications of shunt procedures. SWI sequence detected hemorrhage at multiple sites and helps to unveil the cause of hydrocephalus in many patients. We recommend to include these sequences in the set of routine MRI sequences in cases of hydrocephalus and to follow the newer classification of hydrocephalus as the tool for selection of surgical options.

Financial support and sponsorship

Nil.

Conflicts of interest

There are no conflicts of interest.

References

1. Fishman MA. Hydrocephalus. In: Eliasson SG, Prensky AL, Hardin WB, editor. Neurological Pathophysiology. New York: Oxford; 1978.
2. Carey CM, Tullous MW, Walker ML. Hydrocephalus: Etiology, pathologic effects, diagnosis, and natural history. In: Cheek WR, editor. Pediatric Neurosurgery. 3rd ed. Philadelphia: WB Saunders Company; 1994.
3. Dandy WE, Blackfan KD. Internal hydrocephalus. An experimental, clinical and pathological study. Am J Dis Child 1914;8:406-48.
4. Russell DS. Observation on the pathology of hydrocephalus. Medical Research Council. Special report series No. 265. London: His Majesty's Stationery Office, 1949. p. 112-3.

5. Kandasamy J, Jenkinson MD, Mallucci CL. Contemporary management and recent advances in paediatric hydrocephalus. BMJ 2011;343:146-51.
6. Krishnamurthy S, Li J. New concepts in the pathogenesis of hydrocephalus. Translat Pediatr 2014;3:185-94.
7. Greitz D. Radiological assessment of hydrocephalus: New theories and implications for therapy. Neurosurg Rev 2004;27:145-65.
8. Kartal MG, Algin O. Evaluation of hydrocephalus and other cerebrospinal fluid disorders with MRI: An update. Insights Imaging 2014;5:531-41.
9. Dinçer A, Kohan S, Özek MM. Is all "Communicating" hydrocephalus really communicating? Prospective study on the value of 3D-constructive interference in steady state sequence at 3T. Am J Neuroradiol 2009;30:1898-906.
10. Algin O, Turkbey B. Evaluation of aqueductal stenosis by three-dimensional sampling perfection with application optimized contrasts using different flip-angle evolutions (3D-SPACE) sequence: Preliminary results with 3 Tesla MRI. AJNR Am J Neuroradiol 2012;33:740-6.
11. Jeevanandham B, Kalyanpur T, Gupta P, Cherian M. Comparison of post-contrast 3D-T1-MPRAGE, 3D-T1-SPACE and 3D-T2-FLAIR MR images in evaluation of meningeal abnormalities at 3-T MRI. Br J Radiol 2017;90:20160834.
12. Desai SB. SWI, a new MRI sequence-how useful it is?. Indian J Radiol Imaging 2006;16:13-4.
13. Haacke EM, Mittal S, Wu Z, Neelavalli J, Cheng YC. Susceptibility-weighted imaging: Technical aspects and clinical applications, part 1. AJNR Am J Neuroradiol 2009;30:19-30.
14. Barbosa JH, Santos AC, Salmon CE. Susceptibility weighted imaging: Differentiating between calcification and hemosiderin. Radiol Bras 2015;48:93-100.
15. Ucar M, Tokgoz N, Damar C, Alimli AG, Oncu F. Diagnostic performance of heavily T2-weighted techniques in obstructive hydrocephalus: Comparison study of two different 3D heavily T2-weighted and conventional T2-weighted sequences. Japn J Radiol 2015;33:94-101.
16. Thomas B, Somasundaram S, Thamburaj K, Kesavadas C, Gupta AK, Bodhey NK, *et al*. Clinical applications of susceptibility weighted MR imaging of the brain — a pictorial review. Neuroradiology 2008;50:105-16.
17. Algin O. Evaluation of hydrocephalus patients with 3D-SPACE technique using variant FA mode at 3T. Acta Neurol Belg 2018;118:169-78.
18. Liang L, Korogi Y, Sugahara T, Shigematsu Y, Okuda T, Ikushima I, *et al*. Detection of intracranial hemorrhage with susceptibility-weighted MR sequences. Am J Neuroradiol 1999;20:1527-34.
19. Chavadi C, Bele K, Venugopal A, Rai S. Susceptibility weighted imaging: A novel method to determine the etiology of aqueduct stenosis. IJNS 2016;05:044-6.
20. Tisell M, Almström O, Stephensen H, Tullberg M, Wikkelsö C. How effective is endoscopic third ventriculostomy in treating adult hydrocephalus caused by primary aqueductal stenosis? Neurosurgery 2000;46:104-10.
21. Lapras C, Mertens P, Guilburd JN, Lapras C Jr, Pialat J, Patet JD. Choroid plexectomy for the treatment of chronic infected hydrocephalus. Childs Nerv Syst 1988;4:139-43.
22. Hoppe-Hirsch E, Laroussinie F, Brunet L, Sainte-Rose C, Renier D, Cinalli G, *et al*. Late outcome of the surgical treatment of hydrocephalus. Childs Nerv Syst 1998;14:97-9.